

Beyond harmonic sounds in a simple model for birdsong production

Ana Amador and Gabriel B. Mindlin

*Department of Physics, FCEN, University of Buenos Aires, Ciudad Universitaria, Pab. I (1428),
Buenos Aires, Argentina*

(Received 21 May 2008; accepted 9 November 2008; published online 18 December 2008)

In this work we present an analysis of the dynamics displayed by a simple bidimensional model of labial oscillations during birdsong production. We show that the same model capable of generating tonal sounds can present, for a wide range of parameters, solutions which are spectrally rich. The role of physiologically sensible parameters is discussed in each oscillatory regime, allowing us to interpret previously reported data. © 2008 American Institute of Physics.

[DOI: [10.1063/1.3041023](https://doi.org/10.1063/1.3041023)]

Birdsong has become an animal model system for the study of learned vocalizations with remarkable parallels to human vocal development and sound production mechanisms. For this reason much of the research in this field focuses on the neural basis for motor control and learning. Yet, behavior emerges from the interaction between the central nervous system and its peripheral target organs. In this work we show that the most widely studied songbird, i.e., the Zebra finch, can benefit from nontrivial dynamical properties of its vocal organ to achieve distinctive acoustic features in its song. This work illustrates the need to address simultaneously questions on central motor control and peripheral mechanisms in order to unveil how complex behavior might be achieved.

I. INTRODUCTION

Songbirds are known as an animal model for learning: they require the exposition to a tutor and practicing in order to achieve the proper conspecific songs.¹ For this reason, most of the research in birdsong production focuses on the neural circuitry necessary for its production and acquisition. Yet, behavior emerges from the interaction between a nervous system, a peripheral one, and the environment. Interestingly enough, the avian vocal organ, called the syrinx, presents strong fingerprints of nonlinearities and therefore, the way in which simple physiological instructions will be transduced into sound is not obvious.

In the last years, a number of models have been proposed in order to integrate the large body of experimental work^{2,3} with the expected basic mechanical processes involved in birdsong production.⁴⁻⁶ In this way, a picture starts to emerge in which the roles of different muscles used by a singing bird are unveiled.

The basic mechanism of birdsong production resembles the generation of voiced sounds by humans: the expiratory airflow can drive sustained oscillations of the membranes (vocal folds in humans and labia in birds).^{7,8} Therefore, the models of birdsong production aim at unveiling the main mechanisms and effects responsible for the dynamics of this valve. These models are implemented mathematically, and the synthetic sounds generated by them are compared with

the data. They are realistic enough to be taken as an acceptable tutoring sound by juveniles in controlled experiments.⁹ Nonlinearities in these models can arise as nonlinear restitution forces, dissipative forces that enter during collision between labia, or the dependence of the interlabial pressure with the labial dynamics. If the internal structure of the oscillating labia which modulate the airflow is taken into account, the dimensionality of the models is large enough to display chaotic solutions.^{7,10}

Low dimensional models, on the other hand, have been used to synthesize tonal sounds like the ones produced by Canaries (*Serinus canaria*) or Northern cardinals (*Cardinalis cardinalis*).

Yet, some birds, such as the Zebra finch (*Taeniopygia guttata*) produce spectrally rich sounds. In Fig. 1(a), a representative song of a Zebra finch is displayed.¹¹ Some syllables are nearly tonal (the fundamental frequency is dominant), while in others, the energy is distributed among several supra-harmonics of the fundamental frequency. Recently it was shown that the later sounds have a pulse tone register, and each acoustic pulse is related to a rapid opening of the labia followed by a long closure of the valve to the airflow.¹²

A recent work explored the existence of a relationship between the fundamental frequency and the richness of the spectrum of the syllables in the Zebra finch song. It was found that over a wide range of fundamental frequencies, the higher the value of the fundamental frequency, the poorer its spectral content.¹³ By plotting the spectral content index, a number describing the centroid of the spectrum of an acoustic signal¹⁴ as a function of its fundamental frequency, it was found that for several birds, and all the syllables within their repertoires with a well-defined fundamental frequency, the data were clustered around a simple curve. This suggests the existence of a common mechanism behind the generation of acoustically different sounds.

Beyond high frequency sounds (almost tonal), and spectrally rich harmonic stacks (with fundamental frequencies ranging from 500 to 800 Hz), the Zebra finch song includes noisy notes, for which the computation of a fundamental frequency is not trivial. It was shown that many of those syllables involve the use of the two acoustically independent sound sources that songbirds have.¹⁵ In these cases, the left

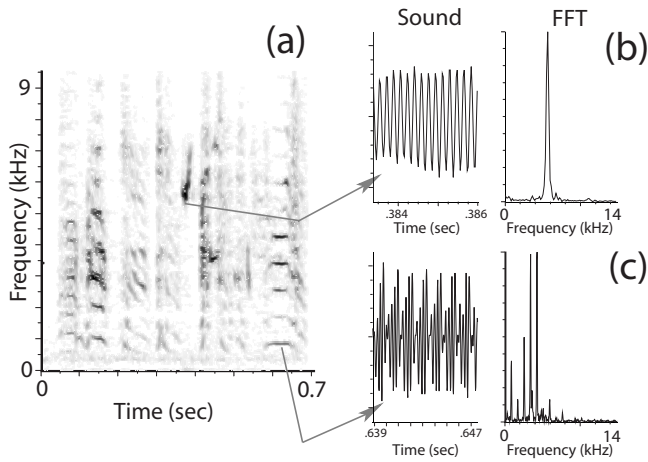


FIG. 1. (a) Sonogram of a typical bout of a Zebra finch. Two segments of the song are analyzed. (b) High fundamental frequency waves are almost tonal, as can be seen directly in the sinusoidal shape of the wave and also in the absence of supra-harmonics in the fast Fourier transform (FFT) analysis. (c) Sounds of low fundamental frequencies are spectrally rich as can be seen in the FFT analysis, where the supra-harmonics have more energy than the fundamental.

and right sides produce acoustically independent sounds with different modulation patterns,¹⁵ giving rise to very complex sounds. These syllables are left aside of our study, which focuses in the question of how a single sound source can generate both tonal sounds and harmonically rich sounds with a well defined fundamental frequency. Recently, the harmonic-to-noise ratio¹⁶ was used to quantify animal sounds which are a mixture of regular components and noisy ones. In the problem of the dog barking, for example, the regular part is likely to be associated with the oscillation of the vocal folds, while the noisy ones are likely to be either due to chaotic motion of the vocal fold tissue¹⁷ or turbulence of the air. In the Zebra finch, these effects might play a role, as well as the acoustical effects emerging from the interaction between the sounds generated by the two independent vocal sources. More work is needed to unveil the processes involved in Zebra finch noisy notes.

From a dynamical point of view, low dimensional models can present periodic oscillations which are spectrally very rich. The aim of this work is to revisit a simple (low dimensional) model for birdsong production, focusing on the search of spectrally rich oscillations. We describe the global bifurcations that give rise to such solutions, and inspect under what conditions they can occur. Bifurcation diagrams in terms of physiological relevant parameters are described, and the acoustic features of the sounds associated with those solutions are discussed.

This work is organized as follows. Section II presents the model. Bifurcation diagrams are discussed in Sec. III. The sounds which can be generated by the described dynamics are presented in Sec. IV. The last section contains our discussion and conclusions.

II. THE MODEL

One of the first low dimensional models for the dynamics of a membrane in an airflow was proposed by Titze⁷ and

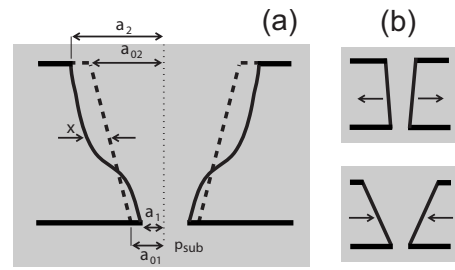


FIG. 2. Flapping model for the labia. (a) The dynamics of the labia is described in terms of the displacement of the midpoint position x . The dashed lines indicate the prephonatory position of the labia, where a_{01} and a_{02} account for the lower and upper distances from the medial point of the tract, respectively. The solid lines represent the surface wave of mucosal tissue traveling upward, where a_1 (a_2) is the half separation between the lower (upper) edges of the labia. In (b) we show the assumed movement of the labia during one cycle of oscillation, which allows self-sustained oscillations to exist: a less divergent profile when the labia move away from each other and a more divergent profile when they approach. The case displayed corresponds to $\Delta a < 0$.

further studied by others.¹⁸ According to this model, the motion of the oscillating tissues is represented as a surface wave propagating in the direction of the airflow. This wave is modeled in terms of two basic modes: a lateral displacement of the tissues, and a flapping like oscillation responsible for an out of phase oscillation of the top and bottom parts of the membranes (see Fig. 2).

The simplest assumption for the existence of self-sustained oscillations is that through a particular phase difference between these modes the system is capable to gain energy in each cycle. The obvious way to accomplish this is to have a convergent profile when the labia move away from each other, and a divergent when they approach. Instead of this configuration, having a less divergent profile when opening than when closing, provides the same effect with not such a dramatic change in the orientation of the profiles [see Fig. 2(b)]. This configuration of profiles allows to have a higher interlabial pressure when the labia are moving apart. In this way, this nonuniform force acting on the membranes allows a net gain of energy in each cycle. The whole movement can be visualized as an upward propagating wave on the membrane.

In order to describe this motion, one can call a_1 (a_2) the half separation between the lower (upper) edges of the labia [see Fig. 2(a)]. Under the hypothesis of a mucosal wave motion on a membrane, these half separations can be written in terms of the midpoint position of a membrane (x) and its velocity (y). If the time that takes the wave to propagate half the vertical size of the labia is τ , the half separations between the edges of the membranes will satisfy

$$a_1 = a_{01} + x + \tau y, \tag{1}$$

$$a_2 = a_{02} + x - \tau y, \tag{2}$$

where a_{01} and a_{02} are the half separations at the rest (nonoscillating) state. Computing the average pressure between the labia,⁷ one obtains

$$p_{av} = p_{sub} \left(1 - \frac{a_2}{a_1} \right), \tag{3}$$

where p_{sub} stands for the sublial pressure. Now it is possible to go beyond the kinetics of the labia to the dynamics. The equations of motion for the variable x is derived taking into account dissipation, elastic restitution, nonlinear dissipation, and read

$$\frac{dx}{dt} = y, \tag{4}$$

$$\frac{dy}{dt} = (1/m) \left(-k(x)x - \beta(y)y - cx^2y + f_0 + a_{lab}p_{sub} \left(\frac{\Delta a + 2\tau y}{a_{01} + x + \tau y} \right) \right). \tag{5}$$

The first term corresponds to a nonlinear restitution force, where $k(x) = k_1 + k_2x^2$. The second term accounts for dissipation, with $\beta(y) = \beta_1 + \beta_2y^2$. The third term is also a nonlinear dissipation that becomes relevant as x takes large values, corresponding to large departures from the rest position. In this way, this position dependent nonlinear dissipation serves to model collisions between labia or with containing walls, either one bounding their motions. The term f_0 accounts for a force that is independent of the labial dynamics, and serves to model active gating.^{5,6} Finally, the last term describes the force f_{lab} acting on the labium due to the interlabial pressure: $f_{lab} = a_{lab}p_{av}$, where $\Delta a = a_{01} - a_{02}$. A slightly simplified version of this model (without nonlinear restitution) was used in Ref. 4 to synthesize canary song. In order to do so, the dynamics of x is used to emulate the modulations of airflow that are responsible for the generation of sound waves. To achieve acoustically realistic sounds, these pressure fluctuations are further filtered emulating the action of a vocal tract.^{4,13} For the case of Zebra finches, this enhances frequencies of the sound source in the range of 3–6 kHz.¹³

The model was further studied by Lucero¹⁸ to investigate oscillation hysteresis. It is interesting to notice that the existence of nonlinear components in the restitution forces for labia was recently found to play an important role in the frequency control of song by a suboscine bird,¹⁹ and qualitatively increases the dynamical possibilities of the model. With its simplicity, this model allowed to identify parameters necessary to account for important acoustic features found in birdsong, such as the temporal evolution of the fundamental frequencies of different syllables.^{4,6} The pressure p_{sub} was identified as the parameter responsible for the onset of the membrane oscillatory motion, and for several oscine birds, k_1 was found to be responsible for the tension of the oscillating labia, which contributes to the value of the fundamental frequency of the uttered sound.

III. BIFURCATION DIAGRAMS

We start our analysis of the dynamics presented by this model with an inspection of its fixed points. They are characterized by $y=0$, and the solutions of

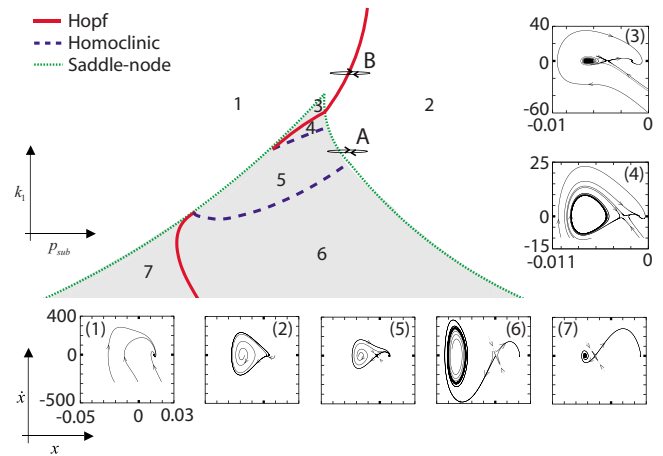


FIG. 3. (Color online) Bifurcation diagram of the model in the (p_{sub}, k_1) parameter space. The shaded region is indicating where three fixed points coexist. The integration of the model for each region is shown in the corresponding insets. In this set of parameters, a Takens–Bogdanov bifurcation occurs, where a saddle-node bifurcation (dotted line) is touched tangentially by a Hopf bifurcation (solid line) and a homoclinic bifurcation (dashed line). Path A passes through a SNILC bifurcation and path B through a Hopf bifurcation. The parameters from Eq. (5) are $a_{lab} = 2.0 \times 10^{-4} \text{ cm}^2$, $m = 0.4 \text{ ng}$, $\beta_1 = 4.44 \times 10^{-5} \text{ dyn s/cm}$, $c = 1.6 \times 10^{-2} \text{ dyn s/cm}^3$, $f_0 = 0.0399 \text{ dyn}$, $\tau = 5.0 \times 10^{-6} \text{ s}$, $a_{01} = 0.1 \text{ cm}$, $a_{02} = 0.11 \text{ cm}$, $k_2 = 400 \text{ dyn/cm}^3$, and $\beta_2 = 4.0 \times 10^{-11} \text{ dyn s}^3/\text{cm}^3$. Finally, the bifurcation diagram corresponds to $k_1 \in [0.16, 0.52] \text{ dyn/cm}$ and $p_{sub} \in [1852, 2084] Pa$.

$$-(k_1 + k_2x^2)x + f_0 + a_{lab}p_{sub} \frac{\Delta a}{a_{01} + x} = 0. \tag{6}$$

In previous works,^{4,5} a fixed point losing its stability in a Hopf bifurcation²⁰ was identified as the basic mechanism leading towards the periodic modulation of airflow, and therefore of sound production. Yet, the model presented here displays a richer set of solutions.

We analyze the bifurcation diagram of our system in terms of the parameters which were found to be relevant for song production.^{4,6} In Fig. 3 we display a region of the parameter space (p_{sub}, k_1) for which three fixed points exist (shaded region). The other parameters were chosen within biologically sensible ones in such a way that $(-f_0 + k_1a_{01}) \approx 0$ and $(p_{sub}\Delta a + f_0a_{01}) \approx 0$, which guarantees a change in the number of solutions of Eq. (6) as k_1 and p_{sub} are slightly changed (see the caption of Fig. 3). Outside this region, a unique fixed point exists. The edges of the cusp shaped region in the parameter space correspond to saddle-node bifurcations (dotted lines in Fig. 3), where a pair of fixed points collide in a unique one with zero linear eigenvalues.

As was mentioned above, the possibility of some of these fixed points undergoing oscillatory instabilities (Hopf bifurcations) was identified as a way to originate periodic motion of the labia, and therefore modulations of the airflow. Hence, it is sensible to perform a linear stability analysis in order to identify the region of the parameter space where these instabilities occur. Computing the eigenvalues of the Jacobian of the system described by Eqs. (4) and (5) we searched for the subset of parameters where the fixed points of our model would present complex eigenvalues with zero real parts, conditions that are necessary for Hopf bifurcations. The continuous curves in the region of (p_{sub}, k_1) under

analysis in Fig. 3 indicate where these conditions are met.

The existence of one-dimensional paths in parameter space where saddle-node (or saddle repulsor) bifurcations take place, and one-dimensional paths where Hopf bifurcations occur, preclude the possibility of rich dynamics when they meet. In Fig. 3 we display a region of the parameter space of our model where different dynamical regimes were found. The different insets display the solutions that we found in each of the regions with different dynamical behavior.

In region 1 of Fig. 3, a unique fixed point is found. Region 3 (inside the shaded region) presents three fixed points: in the transition from region 1 to region 3, a saddle-node bifurcation generates the two additional fixed points. The attractor generated in this bifurcation undergoes a Hopf bifurcation as we enter region 4. The separation between regions 4 and 5 is defined by an homoclinic bifurcation: the limit cycle of region 4 collides with the saddle fixed point. Region 7 is dynamically equivalent to region 3, just as region 6 is equivalent to region 4. Interesting enough, region 5 (separated from regions 4 and 6 by homoclinic bifurcation lines) presents a dynamically rich structure: the unstable manifold of the saddle is part of the stable manifold of the attractor. In this way, when we change the parameters in order to move from region 5 to region 2, a saddle node in a limit cycle bifurcation²¹ (SNILC) takes place.

It is interesting to discuss the degree of generality of the set of solutions found in the analysis here reported. Notice that whenever there are both a one-dimensional set of parameters where a saddle-node bifurcation and a Hopf bifurcation take place, it is generic that they meet. Whenever that occurs, any model can be reduced to a normal form whose dynamics has been thoroughly studied.²⁰ The behavior of any system in the vicinity of the parameter space where a saddle-node and a Hopf bifurcation collide has been studied by Takens and Bogdanov,²⁰ and therefore the solutions found in the numerical simulations of our model are not a specific feature of our model.

Some of the solutions displayed in Fig. 3 have profound effects in terms of our problem. Whenever we abandon region 5 towards region 2, the saddle fixed point and the attractor collide in a saddle-node bifurcation. But as the unstable manifold of the saddle is part of the stable manifold of the attractor, an oscillation is born as the fixed points collide. This oscillation will have important differences with one born in a Hopf bifurcation. In the last case, the oscillation is born with zero amplitude and a finite frequency. On the contrary, an oscillation born in a SNILC bifurcation will present a finite amplitude, and zero frequency. As the parameter is further moved, the frequency will start to increase, but for a region of the parameter space of nonzero measure, the oscillation will present a critical slowing down whenever the variables approach the region of the phase space where the saddle and the attractor collided. The reason is that after the bifurcation there is a saddle-node remnant. The period of the oscillations being born T , in fact, scales as $(a_c - a)^{-1/2}$, where a is the control parameter (the pressure p_{sub} , in our case), and a_c the parameter value at which the bifurcation occurs.²¹ Due to this saddle-node remnant, the labium stays longer time in

one point than Hopf bifurcation case, and moves abruptly. For this reason, the spectral content of the oscillation will be very rich in the vicinity of the parameters where the SNILC bifurcation took place.

We can cross the bifurcation line corresponding to the SNILC by only changing the parameter p_{sub} (sublabial pressure), and the frequency of the oscillations will strongly depend on the distance of the pressure p_{sub} to the bifurcation point. Therefore, the model suggests that it is possible to control the fundamental frequency of the vocalizations with the modulations of the air sac pressure. In Zebra finches, it was reported that low frequency sounds can be produced with no activity of the ventral muscles.²² A plausible interpretation in the framework of this model is that those vocalizations are originated in SNILC bifurcations and the fundamental frequency is only controlled by the air sac pressure.¹³

On the other hand, for other oscine birds, as the Northern cardinals and Brown thrashers (*Toxostoma rufum*), the activity of ventral syringeal muscles strongly correlates with the fundamental frequency of the vocalizations.^{2,6} It was suggested, and mathematical models were consistent with the interpretation, that these muscles change the restitution forces of the oscillating labia, and therefore the larger the activity of those muscles, the larger the frequency of the vocalizations. It is important to notice that the sounds produced by these birds are nearly tonal, so the model used to reproduce the data explored the Hopf bifurcation and not the SNILC. This two behaviors are contemplated in our model, as it is shown in Fig. 3, paths A and B.

As we mentioned before, the reason for choosing the parameters p_{sub} and k_1 in our inspection of the dynamical responses of the system is biased by previous works, where experimentally and theoretically it was shown that p_{sub} was important to overcome dissipation and turning on the oscillations via the energy transfer to the labia, and k_1 correlated with the fundamental frequency of the vocalizations.⁶ There are two other parameters that have an important effect in the solutions of our model. The term f_0 corresponds to a force independent of the labial dynamics, and it has been interpreted in terms of the action of active gating by oscine birds (controlled by dorsal syringeal muscles).^{2,5} Mathematically, this term avoids oscillations by moving the fixed point to regions of the space where dissipation is too high (either pushing the labia together, or contracting them towards the containing walls). In terms of our model, the increase of f_0 does in fact turn oscillations off. In Fig. 4 we show how the bifurcation diagram is translated to the right as f_0 is increased. In this way, if the system is in a region of the parameter space where it is oscillating (region 2 in Fig. 3), it is possible to increase f_0 until entering to the region 1 where no oscillations occur.

In our model, the parameter Δa , describes the shape of the prephonatory position. The rich structure of fixed points which was ultimately responsible for the appearance of SNILC bifurcations occurs if Eq. (6) presents more than one zero. As in our model $p_{\text{sub}} > 0$, if $\Delta a < 0$ then Eq. (6) will have three roots. Besides this, it must be taken into account that the existence of the cusp is a necessary condition but not sufficient to have a SNILC bifurcation. In order to have this

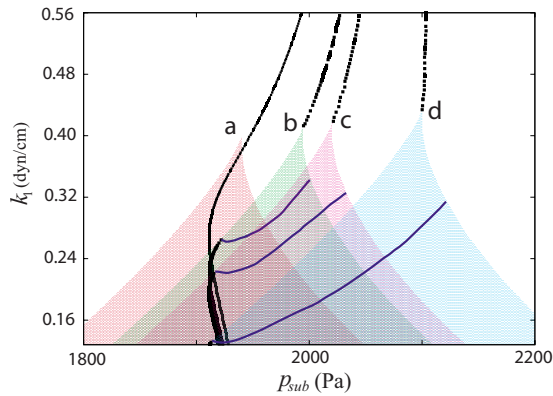


FIG. 4. (Color online) Bifurcation diagrams for different values of f_0 . As in Fig. 3, the shaded regions correspond to parameter values where three fixed point exist. Hopf bifurcation curves are shown with black squares and homoclinic bifurcation curves with blue lines. The values of f_0 used are: (a) $f_0=0.0388$ dyn, (b) $f_0=0.0399$ dyn, (c) $f_0=0.0404$ dyn, and (d) $f_0=0.0420$ dyn.

bifurcation, it is needed that the Hopf line touches the saddle-node line in such a way that the regions 2 and 5 are adjacent and the borderline separating these regions is a saddle-node bifurcation (as is shown in Fig. 3). For $\Delta a > 0$, only one fixed point exists, and the only qualitative change that is possible to find as the parameters are changed is a Hopf bifurcation giving rise to nearly tonal oscillations. In this way, the same model is capable of presenting the rich dynamics associated with spectrally rich sounds and tonal sounds.

IV. PATHS IN PARAMETER SPACE

In previous works, computational models were used to synthesize birdsong.^{4,5} Slow parameter changes in pressure were used to place the model in a region of the parameter space where oscillations would occur, and eventually to return the system to a region of nonoscillating solutions. The acoustic features of the sounds would depend on the values of the other parameters, which could also change slowly or remain fixed. Actually, some of these models were driven by experimentally recorded parameters (as the air sac pressure and activity of ventral syringeal muscles) and used to generate synthetic sound.⁶ In this section we explore the parameter space through different paths, in order to describe acoustically the sounds generated. Since new dynamical regimes exist, new acoustic features are expected.

In Fig. 5 we illustrate our results. In panel (a), we show the sonogram¹¹ of the synthetic song generated when the parameters are moved along the closed path A displayed in Fig. 3. This path consists of a cyclic movement of the parameter p_{sub} [Fig. 5(c)] for a fixed value of k_1 . The chosen value of k_1 guarantees that the oscillation starts in a SNILC bifurcation. As the system enters the region of the parameter space where the oscillations take place, sound is generated. As in Refs. 4, 5, and 8, the oscillations of the labia are used to generate an oscillating airflow which is finally used to synthesize sound. Notice the rich spectral content of the sound, indicated by many dark lines in the sonogram. In the inset of Fig. 5(a) we illustrate the generated time series data.

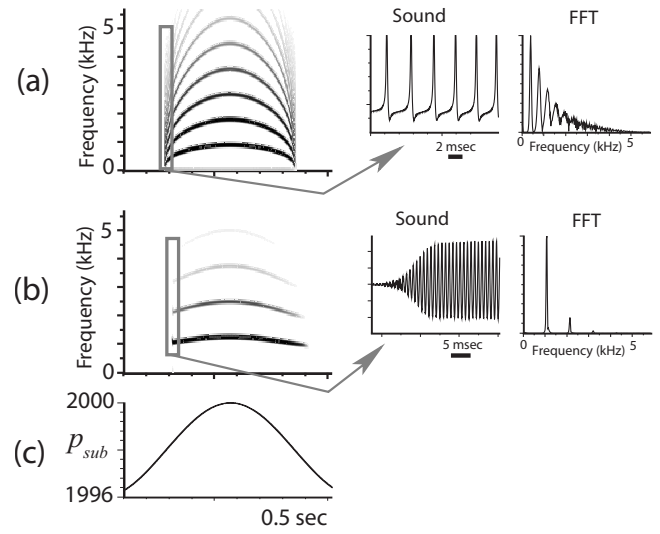


FIG. 5. Synthetic sounds generated with the model. The sound in (a) is obtained using path A in the parameters space shown in Fig. 3. This corresponds to a fixed value of k_1 ($k_1=0.36$ dyn/cm) and p_{sub} , as shown in (c), that allows the system to go through a SNILC bifurcation. The inset shows a segment of the sound wave and its corresponding fast Fourier transform to analyze the energy of the harmonics. In (b) we show the analogous for a different value of k_1 ($k_1=0.42$ dyn/cm), corresponding to path B in Fig. 3. The amplitude of the sound wave has the characteristic shape of a Hopf bifurcation. The comparison of both FFT shows that the signals born in a SNILC bifurcation have a richer harmonic content than those born in a Hopf bifurcation, which correspond to quasi-tonal sounds.

Its shape is very different from a simple harmonic oscillation, which is also clear from its spectrum. It is illustrative to compare these results with the sound generated using the path labeled B in Fig. 3, where the only changed parameter is k_1 and the variation of p_{sub} is the same of path A. In this case [Fig. 5(b)], the system undergoes a Hopf bifurcation, where a harmonically poor oscillation is born. The sonogram displays, for the same resolution, a smaller number of curves, the shape of the oscillations resembles simple harmonic ones (of growing amplitude as expected in a Hopf bifurcation as the parameters are increased), and finally the spectrum of a segment shows supra-harmonic peaks of small amplitude.

The synthetic sounds generated in Fig. 5 illustrate how the two different dynamical mechanisms for generating oscillations discussed in this work can account for the spectral features of the representative syllables described in Fig. 1. As in the syllable displayed in Fig. 1(b), the synthetic sounds originated in a Hopf bifurcation have almost all their energy in the fundamental frequency. The synthetic sounds originated at a SNILC [Fig. 5(b)], will have a rich spectral content. In the experimental data [Fig. 1(c)], beyond a rich spectrum we can observe the influence of the vocal tract which emphasizes the harmonics between 3 and 6 kHz (an effect not considered in our model).

Notice that in the sonogram of Fig. 5(b), there is still a small dependence of the fundamental frequency with the pressure. This is a consequence of the nonlinear term in the restitution force. As the pressure is increased, the fixed point moves away from its rest position. In this way, with a fixed value of k_1 we obtain modulations in the fundamental frequency of the sound trough modulations in the pressure. This

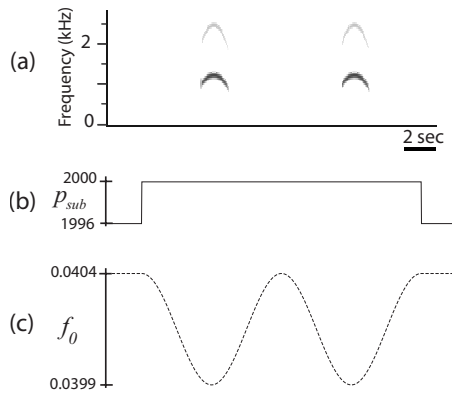


FIG. 6. Polysyllable sound (a) generated with one pressure pulse (b). Even for high values of the pressure, the oscillations can still be prevented increasing the value of f_0 . In other words, the phonation threshold changes with f_0 (see also Fig. 4). The values of the parameters are the same as in Fig. 3, with $k_1=0.42$ dyn/cm.

effect was already discussed in the framework of the sound production of a suboscine bird (the Great Kiskadee), which does not require an active control of ventral muscles to produce variations of the fundamental frequency of its vocalizations.¹⁹ In some oscine species, where wide excursions in fundamental frequency is an appealing characteristic of their vocalizations,¹ it is likely that they require more than this small dependence of frequency with air sac pressure, and an active control through ventral syringeal muscles is to be expected.

The last characteristic of the song that we synthesize is the capability of uttering multiple syllables with the same pressure pulse. In Zebra finch it is observed that there are some syllables (continuous lines in a sonogram) that are produced within an expiratory pulse.¹³ Since it was reported the role of the dorsal syringeal muscles is adduction,² the simplest interpretation is that the bird is using the dorsal muscles to actively close the tract and prevent oscillations of the labia. In terms of the model, this effect is described by the term f_0 . In Fig. 6 we show how this can be synthesized: during a unique pressure pulse, the increase of the value f_0 turns the oscillations off.

V. CONCLUSIONS

In this work, we have studied the solutions of a simple model of birdsong production. The introduction of a nonlinear component of the restitution force allowed us to find a rich variety of dynamical regimes. Beyond the oscillations born in a Hopf bifurcation, which was already reported as a plausible mechanism for the onset of tonal sounds, we found a variety of different dynamical regimes. Their existence, in the model, depend on the prephonatory shape of the labial configuration. This prephonatory shape is not only the initial condition but defines an average convergent or divergent profile as the dynamics of x defines only a small departure from the rest position.

One of the most interesting scenarios found in the model was the existence of SNILC bifurcations, where a saddle fixed point whose unstable manifold is part of the stable manifold of an attractor, collides with it. Oscillations of zero

frequency are born at the bifurcation. As the bifurcation parameter is slightly moved away into the region of parameter space where oscillations occur, the frequency increases. These oscillations are spectrally very rich, generating sounds with non tonal features. In this way, different spectral features of sound originate in the dynamics of the avian vocal organ.

The nonlinear nature of the avian vocal organ was already reported to have important consequences in the sound it produces, from subharmonic solutions,²³ to nontrivial transduction of pressure into frequency,¹⁹ among other effects. In this work we describe the dynamics behind the relationship between fundamental frequency and spectral content¹³ in some sounds (those originated at SNILC bifurcations).

In the study of birdsong, a large effort is made in order to understand the neural basis of the motor commands responsible for the different acoustic features of the song. Yet, behavior emerges from the interaction of a nervous system, a peripheral system, and environment. This study illustrates that many features might not require separate instructions, but are linked by the nature of the dynamical solutions of the peripheral system.

ACKNOWLEDGMENTS

We thank Franz Goller and Jacobo Sitt for useful discussions. This work was partially funded by UBA, CONICET, and Fundación Antorchas.

¹H. S. Peter Marler, *Nature's Music: The Science of Birdsong* (Elsevier Academic, San Diego, 2004).

²F. Goller and R. A. Suthers, *J. Neurophysiol.* **75**, 867 (1996).

³R. A. Suthers and S. A. Zollinger, *Ann. N.Y. Acad. Sci.* **1016**, 109 (2004).

⁴T. Gardner, G. Cecchi, M. Magnasco, R. Laje, and G. B. Mindlin, *Phys. Rev. Lett.* **87**, 208101 (2001).

⁵R. Laje, T. Gardner, and G. B. Mindlin, *Phys. Rev. E* **65**, 051921 (2002).

⁶G. B. Mindlin, T. J. Gardner, F. Goller, and R. Suthers, *Phys. Rev. E* **68**, 041908 (2003).

⁷I. R. Titze, *J. Acoust. Soc. Am.* **83**, 1536 (1988).

⁸G. B. Mindlin and R. Laje, *The Physics of Birdsong* (Springer, Berlin, 2005).

⁹T. J. Gardner, F. Naef, and F. Nottebohm, *Science* **308**, 1046 (2005).

¹⁰H. Herzel, D. Berry, I. Titze, and I. Steinecke, *Chaos* **5**, 30 (1995).

¹¹A sonogram is a computation of the fundamental frequency of a sound along time. It is the standard way to represent a song (see Ref. 8).

¹²K. K. Jensen, B. G. Cooper, O. N. Larsen and F. Goller, *Proc. R. Soc. London, Ser. B* **274**, 2703 (2007).

¹³J. D. Sitt, A. Amador, F. Goller, and G. B. Mindlin, *Phys. Rev. E* **78**, 011905 (2008).

¹⁴G. Agostini, M. Longari, and E. Pollastri, *EURASIP J. Appl. Signal Process.* **1**, 5 (2003).

¹⁵F. Goller and B. G. Cooper, *Ann. N.Y. Acad. Sci.* **1016**, 130 (2004).

¹⁶T. Riede, H. Herzel, K. Hammerschmidt, L. Brunnberg, and G. Tembrock, *J. Acoust. Soc. Am.* **110**, 2191 (2001).

¹⁷I. Tokuda, T. Riede, J. Neubauer and M. Owren, *J. Acoust. Soc. Am.* **111**, 2908 (2002).

¹⁸J. C. Lucero, *J. Acoust. Soc. Am.* **105**, 423 (1999).

¹⁹A. Amador, F. Goller, and G. B. Mindlin, *J. Neurophysiol.* **99**, 2383 (2008).

²⁰J. Guckenheimer and P. Holmes, *Nonlinear Oscillators Dynamical Systems and Bifurcation of Vector Fields* (Springer, Berlin, 1990).

²¹S. Strogatz, *Nonlinear Dynamics and Chaos with Applications to Physics, Biology, Chemistry, and Engineering* (Westview, Boulder, CO, 2000).

²²D. Vicario, *J. Neurobiol.* **22**, 63 (1991).

²³M. S. Fee, B. Shraiman, B. Peseran, and P. P. Mitra, *Nature (London)* **395**, 67 (1998).